CONTROLS ON pH AND PYRITE OXIDATION PATHWAYS ACROSS THE PHREATIC SURFACE OF A COAL WASTE DEPOSIT IN SOUTHWEST[1]

D.S. Hardisty[2], G.A. Olyphant[3], and L.M. Pratt[3]

Abstract: During acid mine drainage (AMD) generation, the factors controlling pH and pyrite oxidation can differ between the saturated and unsaturated zones. These differences, however, may not always be considered during field-scale remediation efforts. At an unreclaimed coal waste deposit in southwest Indiana, preliminary studies have identified a horizontal pH gradient that increases from 2.8 to 6.5 along a 90 meter shallow groundwater flow path. This site provides a unique opportunity to determine pyrite oxidation pathways under varying conditions within both the saturated and unsaturated zones of coal mine refuse being subjected to weathering processes. Vertical profiles of pore-water were obtained using diffusion-controlled dialysis membrane samplers installed across the phreatic surface. Samples were collected at 2 cm intervals from the ground surface to a depth of 40 cm with the bottom 10 cm being fully saturated. Samples collected during the summer reveal a linear trend with respect to pH and depth with pH values of approximately 2.5 near the surface to 3.4 at the base of the profile. Concentrations of sulfate (SO_4^{2-}) and iron (Fe-total) during the summer are highest near the surface and in the case of Fe, decrease by an order of magnitude at the bottom of the profile. Samples collected during the autumn show that within the saturated zone, ferrous iron (Fe^{2+}) concentrations are elevated relative to ferric iron (Fe^{3+}), but Fe^{3+} increases with decreasing pH. This indicates that atmospheric oxygen is the limiting factor in pyrite oxidation both through direct oxidation of pyrite and through the oxidation of Fe^{2+} to Fe^{3+} that can then oxidize pyrite in both saturated and unsaturated conditions at lower pH values. These results imply that an increase in the thickness of the saturated zone can act as a control on acidity generation by preventing positive feedback cycling of Fe^{3+} to oxidize pyrite.

Additional Keywords: Fe cycling, peeper

---

[1] Paper was presented at the 2010 National Meeting of the American Society of Mining and Reclamation, Pittsburgh, PA ***Bridging Reclamation, Science and the Community*** June 5 - 11, 2010. R.I. Barnhisel (Ed.) Published by ASMR, 3134 Montavesta Rd., Lexington, KY 40502.

[2] Dalton Hardisty*, Research Assistant, Indiana Geological Survey, Center for Geospatial Analysis [3]Greg Olyphant, Professor and Research Hydrogeologist, Indiana University, Department of Geological Sciences, Center for Geospatial Data Analysis, 1001 East 10th Street, Bloomington, IN 47405; Lisa Pratt, Professor, Department of Geological Sciences, Indiana University, 1001 East 10th Street, Bloomington, IN 47405

Proceedings America Society of Mining and Reclamation, 2010 pp 434-448
DOI: 10.21000/JASMR10010434
http://dx.doi.org/10.21000JASMR10010434

INTRODUCTION

Hydrochemical conditions at an abandoned slurry deposit, located in Dugger, IN, (Fig. 1) were monitored during the period of 2007-2009 as part of a reclamation feasibility study. The generation of acidic groundwater in the coal waste and its seepage into adjacent Mud Creek was a major concern. The present study is driven by the premise that a better understanding of the active sites of pyrite oxidation in relation to hydrologic conditions at this and other abandoned mine lands sites can lead to more effective reclamation strategies that involve passive treatment of acidic groundwater. Huminicki and Rimstidt (2009) demonstrated with laboratory experiments that where low rates of groundwater flow exist, increasing the pH of waters in contact with pyrite, could allow Fe oxyhydroxide minerals to precipitate and coat could pyrite grain surfaces. As the coating thickness increased it acted as a barrier to oxidation. Other studies by Williamson and Rimstidt (1994) show that oxidation rates of pyrite in saturated conditions are slower than those that occur in unsaturated conditions after extended time periods. These studies and others present effective strategies to minimize pyrite oxidation, but in each case consideration must first be given to determining pyrite oxidation pathways and potential within both the saturated and unsaturated zones in areas scheduled for reclamation.

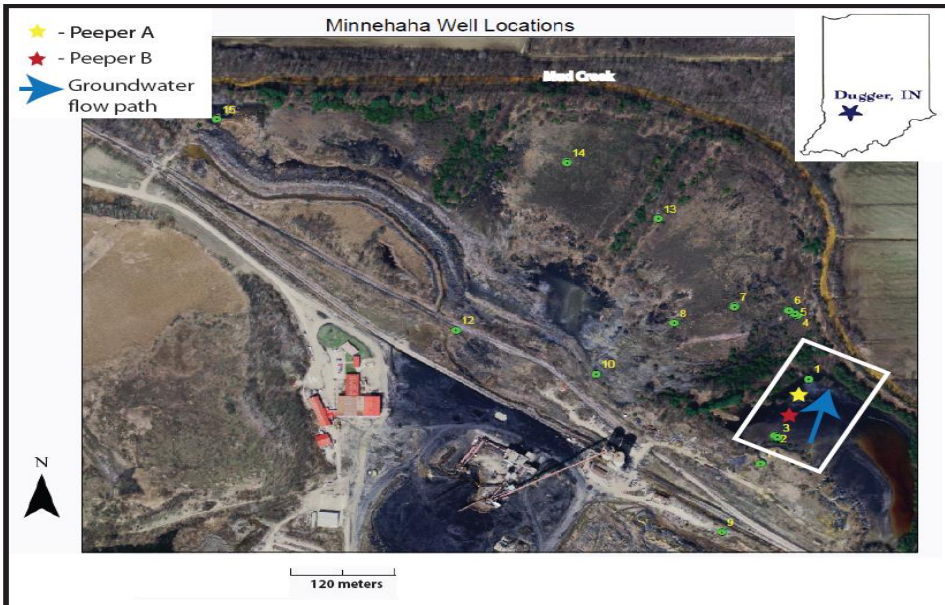

Figure 1. Site map showing well locations, peeper locations, and groundwater flow path within the sampling area. Minnehaha is located in Dugger, IN.

Background Data

Monitoring wells and instruments for monitoring hydrologic fluctuations were installed in the waste deposit (Table 1) and sampling devices were emplaced to collect pore water samples from both the saturated and unsaturated zone along a known groundwater flow path in an effort to delineate pyrite oxidation sources and infer geochemical processes. Water table elevations revealed a down slope gradient from well 3 to 1 (Table 1), indicating the groundwater flow direction within the tailings pond (Fig. 1)

Table 1. Minimum, average, and maximum unsaturated zone thickness for the tailings pond located in Minnehaha.

unsaturated thickness (m)	Well 1	Well 3
average	0.70	0.33
minimum	0.08	0.0
maximum	1.21	0.83

Preliminary monitoring indicated that during 2008 the water table occupied the upper 18 cm of the surface 40% of the time at well 3 and 5% of the time at well 1 (Table 2). At a depth of 41 cm, (approximate average water table depth) the sediments surrounding well 3 were fully saturated 60% of the time. The narrow unsaturated zone thickness (Table 1) in the refuse deposit allows for quick recharge of the water table in response to rain events, with the water table often intersecting the surface. The variability in water-table elevation in the upper portion of the coal refuse results in pyrite being exposed to both saturated and unsaturated conditions during the year. Samples of groundwater from wells 1 and 3 during the summer of 2009 exhibited pH values ranging from 2.5 to 6.0 across the flow path.

Oxidation rates of pyrite differ under saturated and unsaturated conditions (Jerz and Rimstidt, 2004; Williamson and Rimstidt, 1994) and in response to mineral precipitation that affects exposure of unweathered pyrite surfaces to oxidants such as Fe^{3+} (Huminicki and Rimstidt, 2009). Preliminary data from core samples collected near wells 1 and 2 indicate that pyrite concentrations in the uppermost meter of the refuse is 0.37 wt% near well 1 and 1.17 wt% near well 3. These values reveal that there is potential for both current and future generation of

acidity in response to varying oxidation pathways within both the saturated and unsaturated zones of the refuse.

Table 2. Percentage of hours during 2008 that various depth intervals were saturated near wells 1 and 3 at Minnehaha in Dugger, IN.

Saturated thickness (m)	Well 1 (% of hours saturated)	Well 3 (% of hours saturated
≤ 0.41 (Peeper depth)	22.30	58.74
≤ 0.18	4.43	40.64
= 0	0.00	16.21

METHODS

Hydrologic data were obtained from monitoring wells distributed throughout the site (Table 1). Emphasis was placed on data from wells 1 and 3 due to their presence along the flow path and proximity to the pore water sampling sites. Pressure transducers were installed in wells 1 and 3 and measurements of groundwater level recorded hourly. Monitoring wells were drilled to bedrock, and in each case the screens were placed in the lower portions of the well.

Diffusion-controlled dialysis membrane samplers, "Peepers" were installed at a depth of 41 cm below the surface at the two locations indicated in Fig. 1. This allowed collection of in-situ pore water samples through a zone that intersected the phreatic surface in the refuse (Fig. 2). Previous studies have used peepers to successfully obtain pore water profiles, including monitoring of constructed wetlands (Fortin et al., 2000) as well as other environments where acid sulfate soil development is occurring (Smith and Melville, 2004; White et. al, 2008). The peepers at Minnehaha are being used to collect pore waters seasonally over the duration of an annual hydrologic cycle and the subsequent analyses of the samples allow evaluation of Fe redox cycling and its interaction with atmospheric oxygen and sulfide minerals in the refuse. These data are also used to determine the oxidation potential of both the saturated and unsaturated zones of the coal refuse.

The diffusion-controlled dialysis membrane samplers (Fig. 3) have been used to collect pore water samples on two occasions thus far. The first collection period occurred during the early

summer of 2009 and the second during the autumn of 2009. Sampling collection dates were chosen based on a predicted increase in the saturated zone thickness of the coal refuse from summer to fall. Before placement in the field, each of the 41 peeper cells were completely filled with deionized water (15 mL per cell), and then covered with a supor polyethersulfone membrane. Peepers were placed vertically in the coal refuse to a depth of 41 cm. The deionized water within the peepers was allowed to equilibrate with the coal refuse pore water for 21 days in the summer and autumn. This duration was chosen based on preliminary studies of equilibrium rates of the peepers with surrounding waters as well as estimates from previous studies (Fortin et al., 2000; White et al., 2008). Following the equilibration period, the summer samples were immediately placed in coolers containing liquid nitrogen absorbed within Styrofoam to act as a coolant during transportation.

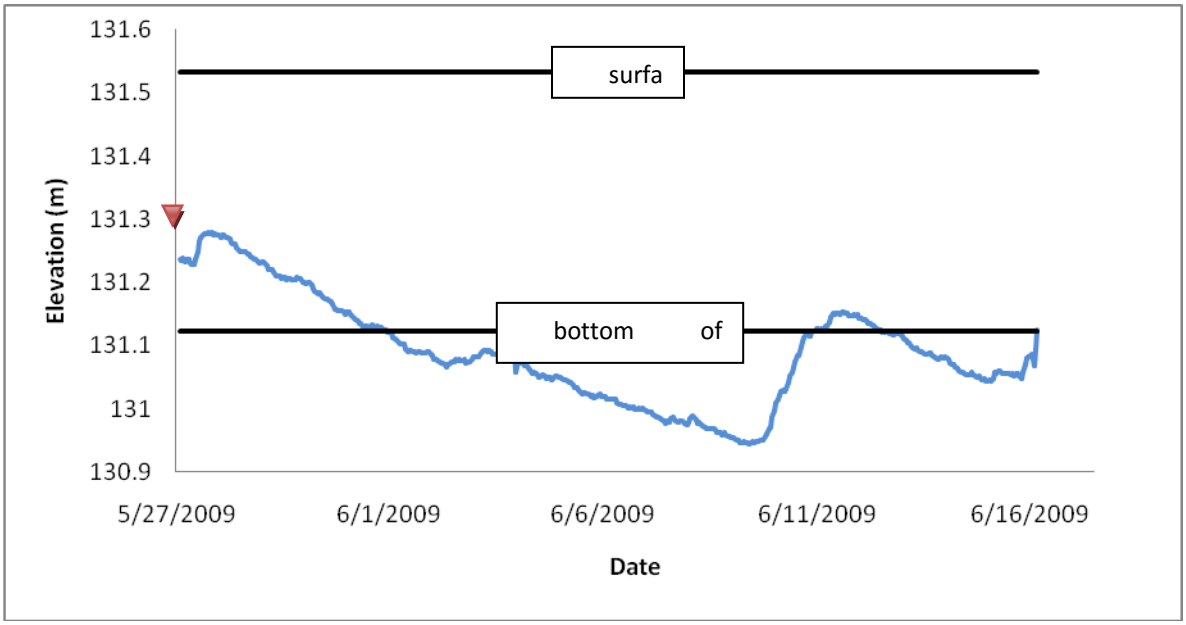

Figure 2. Hydrograph of water level data from Well 1 (corresponding to peeper location A) showing groundwater elevation in relation to the coal refuse surface and lowest cell depth of peeper location A.

Once in the lab, aliquots of water from each cell were removed by perforating the membrane with needle tipped syringes and extracting the liquid. During the autumn sampling, the aliquot separation procedure was carried out in the field immediately following extraction of the peepers from the coal refuse. For both the summer and autumn sampling periods, pore water from adjacent peeper cells were combined as necessary to ensure sufficient water volume for each analysis and samples were stored at a temperature of 4°C prior to analysis.

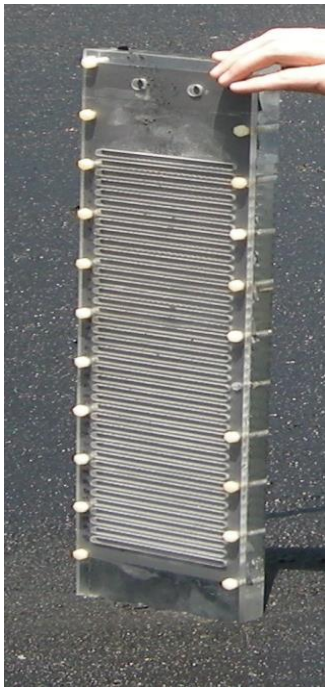

Figure 3. Diffusion-controlled dialysis membrane sampler (peeper). The peeper contains 41 cells separated by 1 cm each. Each cell consists has a volume of 15 mL.

Each sample was divided into two subsamples: one for anions and the other for cations. The minimum water sample volume required is 0.5 mL for use with the *IC25 Ion Chromatograph* (used for anions) and 0.5-3 mL for *AAnalyst A800 Atomic Absorption Spectrometer* (used for cations). Cations analyzed include calcium (Ca^{2+}), magnesium (Mg^{2+}), sodium (Na^{+}), potassium (K^{+}), and Fe-total. Anion analytes include SO_4^{2-}, bromine (Br^{-}), phosphate (PO_4^{3-}), fluorine (F^{-}), chlorine (Cl^{-}), nitrate (NO_3^{-}), and nitrite (NO_2^{-}). Autumn samples were also analyzed for Fe^{2+} and Fe^{3+} concentrations through the use of an *Dionex© ICS-2000 Ion Chromatograph System*. Measurements of pH and Eh were performed through the use of a calibrated ORION model 250A pH and Eh meter on remaining water not needed for anion or cation determination.

Each cation sample was prepared for Atomic Absorption analysis by adding Ultrapure 95% nitric acid to bring the sample pH below 2. The sample was then prepared for analysis by making up 50 mL solution of sample and 0.02% HNO_3 acid (1:50 ratio). A 2-3 mL aliquot was taken from each solution and loaded into the AAS. Samples were analyzed according to the *Fisher Scientific* lab manual procedure. Working standards were diluted from single element references from *Fisher Scientific* and were used to bracket the analysis of samples for calibration purposes.

Anion samples were diluted with deionized water (1:50 ratio) before analysis with an ion chromatograph. For calibration purposes, sample analyses were bracketed with working standards of Na and K salts as suggest by *Dionex.* Instrument procedures for *IC25 Ion Chromatograph* were followed as given in the lab manual.

Samples analyzed for Fe^{2+} and Fe^{3+} concentrations were diluted using deoxygenated water (1:10 ratio).

RESULTS

Summer

Figures 4a and 4b are plots of pH as a function of depth at the two peeper sites. Both profiles show a linear trend of increasing pH with depth. This trend is consistent with the Fe concentration curves that show decreased Fe with depth (Fig. 5). Increased pyrite oxidation closest to the surface would generate both acidity and increased Fe through the following reaction:

$$FeS_2 + 7/2O_2 + H_2O \rightarrow Fe^{2+} + 2SO_4^{2-} + 2H^+ \quad \textbf{(1)}$$

Both pH profiles show a similar value of pH (≈3.4) at a depth of 40 cm which is within the saturated zone, but surface values differ with a value of 2.6 at peeper location A (Fig. 4a) and a value of 2.8 at peeper location B (Fig. 4b). The slope of the pH trend line for peeper location B indicates a steeper pH gradient than at peeper location A. The unsaturated zone is also thicker at location A than at location B.

Fe concentrations from peeper location A show a distinct initial increase with depth (Fig. 5). The increasing trend ends near a depth of 13 cm where the Fe concentration peaks at 370 ppm. Below 13 cm Fe concentration remains above 250 ppm until a depth 25 cm where a sharp, order of magnitude, decrease in Fe concentrations occurs. Concentrations of Fe for peeper location B show a maximum value of 103 ppm and a minimum value of 10 ppm. This range of values is considerably less than the range from pore waters at peeper location A. Also note that the depth profile of Fe concentration versus depth for peeper location B showed no distinct systematic trend.

Sulfate and calcium concentrations at peeper location A for the summer sampling showed a similar trend with decreasing values until a depth of approximately 25 cm when the concentrations begin to increase until the bottom of the profile (Fig. 5). Sulfate concentrations

ranged from 1,500-3,500 ppm for peeper location A (Fig, 5) and 1,500-2,250 ppm for peeper location B. Calcium concentrations at peeper location A were also elevated in comparison to peeper location B with a maximum concentration of 515 ppm at location A and 154 ppm at location B (Fig, 5).

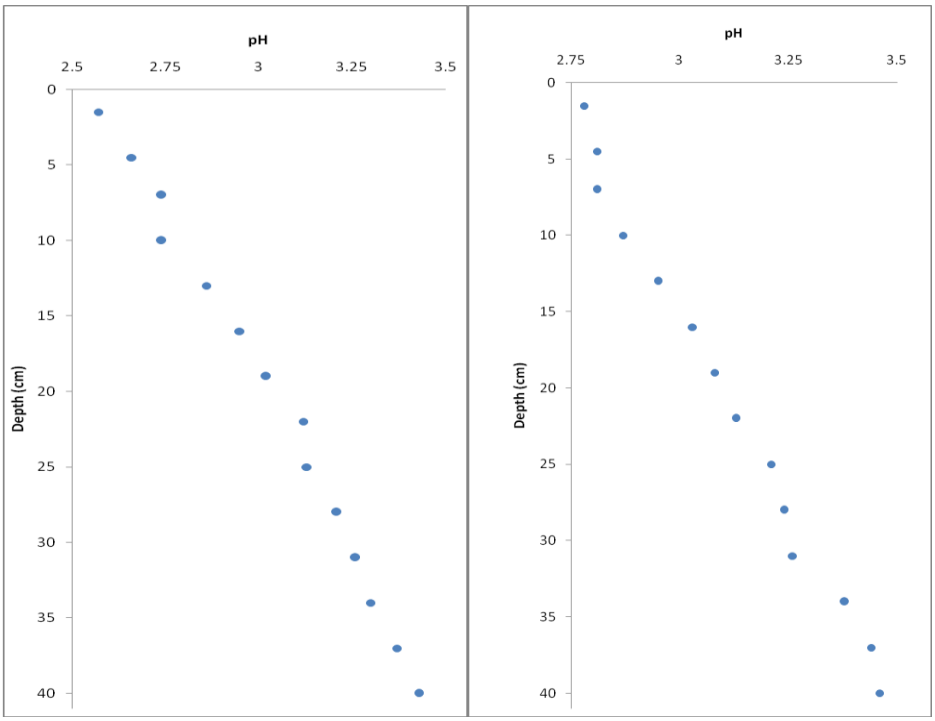

a.) **b.)**

Figure 4. Plots of pH versus depth for samples collected in summer, 2009. **a.)** Peeper location A **b.)** Peeper location B

Saturation Index calculations using PHREEQC (Parkhurst and Appelo, 1999), with the MINTEQ database, showed that the majority of pore waters were saturated with gypsum and anhydrite during the summer sampling period. Evaporation during the sampling time period would concentrate ions in pore waters near the surface within the unsaturated zone, allowing for mineral precipitation. Other secondary minerals commonly found in acidic mine waters such as Fe oxyhydroxides and jarosite were undersaturated. Precipitation of gypsum is favorable over jarosite because Ca^{2+} and SO_4^{2-} are the most prevalent ions in the pore waters whereas jarosite requires Fe^{+3} which is limited in solution in relation to Ca^{+2}. It should be noted that saturation indices are not a direct indication that mineral precipitation is occurring, but instead indicate the potential for precipitation by providing evidence of the thermodynamic stability of the mineral.

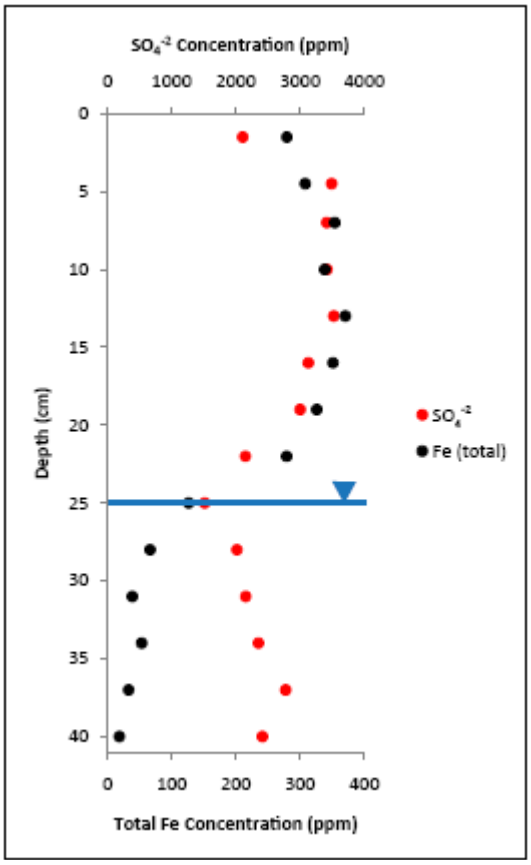

Figure 5. Depth profile of total Fe concentrations taken from peeper location A during the summer sampling period.

Autumn

Samples of pore water collected in the autumn exhibit pH profiles that are nonlinear. At peeper location A the trend of pH with depth is inverse of that observed during the summer sampling period (Fig. 6a). At a depth of approximately 27 cm the pH begins to increase until a depth of approximately 33 cm where the pH again begins to decrease. This trend is distinctly different than that observed at peeper location B where the pH at the surface is 3.82 compared to 3.41 at peeper location A (Fig. 6b). Values of pH decrease to a depth of approximately 33 cm where they begin to become stable at a pH of approximately 3.07. This depth of stability approximately corresponds to the depth of the water table at peeper location B. The pH trends for the autumn samples differ from those of the summer samples in that they are nonlinear with pH decreasing rather than increasing with depth.

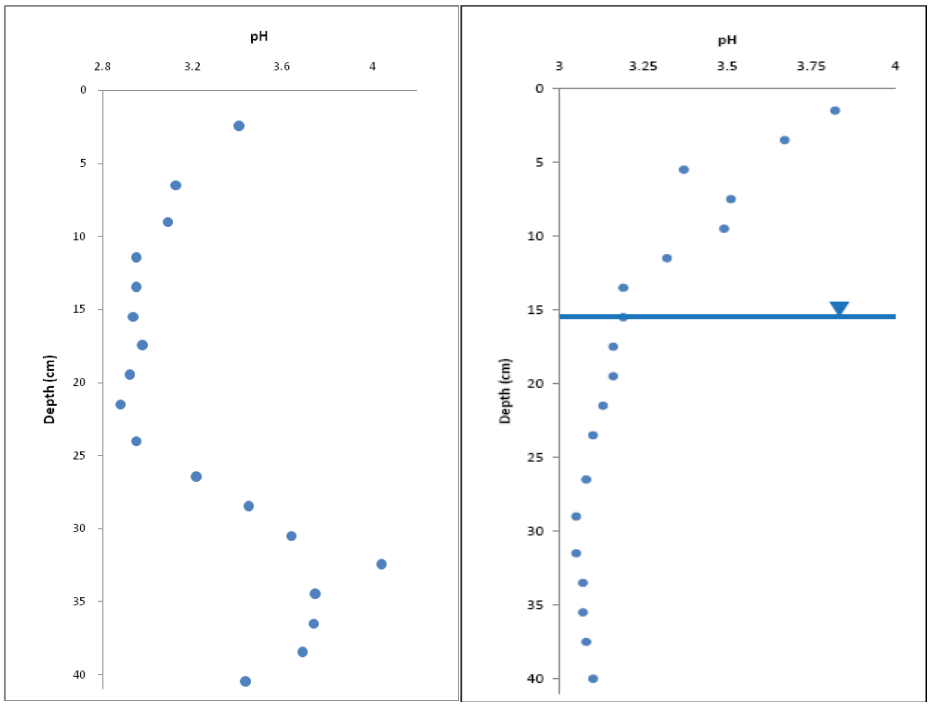

a.) **b.)**

Figure 6. Plots of pH versus depth for samples collected in the autumn of 2009. **a.)** Peeper location A. **b.)** Peeper location B.

Samples collected during the autumn were analyzed for both Fe^{2+} and Fe^{3+} iron concentrations to interpret Fe redox conditions. The total Fe concentrations at peeper location A are higher than at peeper location B (Fig. 7). The major difference between the two profiles is that pore water from peeper location A is dominated by Fe^{3+} iron while the pore water at peeper location B is dominated by Fe^{2+} iron. As in the summer sampling, the unsaturated thickness is greater at peeper location A than at peeper location B. Depth to water measurements show that the water table never reached the bottom of the peeper (depth of 40 cm) at peeper location A, but rose to approximately 18 cm below the surface at peeper location B. Exposure to atmospheric oxygen oxidizes Fe^{2+} to Fe^{3+}, but when oxygen is limited, microbes present at low pH's oxidize Fe^{2+} much more rapidly than dissolved or atmospheric oxygen. The presence of a system only partially dominated by Fe^{3+} has significance because of the role of Fe^{3+} as the principal oxidant in waters with a pH<4 (Huminicki and Rimstidt, 2004) such as those observed in this study.

As in the summer, the total Fe concentrations are also different in the autumn peeper samples between the peeper locations A and B. Shown in Fig. 7, the autumn Fe concentrations have a characteristic peak that occurs at approximately 24 cm depth for peeper location A and at a depth

of approximately 35 cm for peeper location B. These are both deeper than the peaks that occurred in the summer. Also, the concentrations of Fe are significantly less in the autumn sampling than in the summer sampling. The maximum Fe-total concentration from the autumn sampling is 47 ppm, an order of magnitude lower than maximum values found for the summer sampling. This is likely a result of evaporation during the summer concentrating ions in pore waters, followed by dilution during autumn precipitation events (Nordstrom et al., 2000). In both the summer and autumn sampling events the peepers located nearest well 1 (peeper location A) had the highest Fe concentrations. In both cases the unsaturated zone was thicker near well 1, making concentrated evaporation a possible explanation for the increase Fe concentrations.

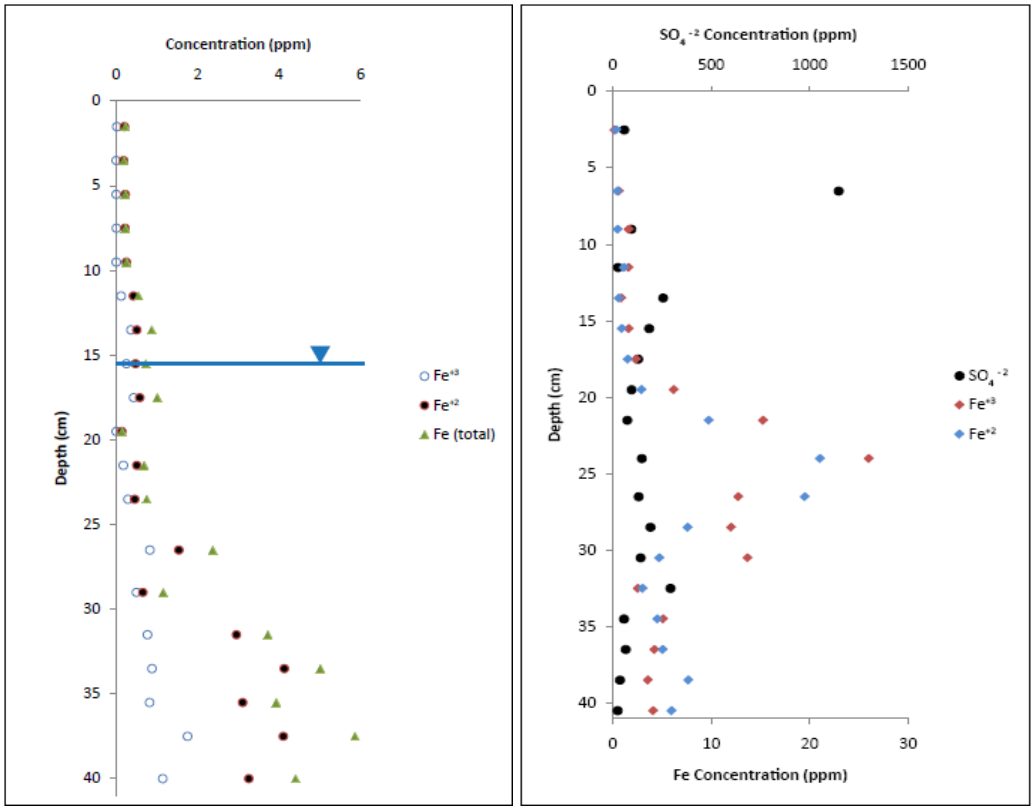

a.) **b.)**

Figure 7. Plots showing the ferrous Fe, ferric Fe, and the sums of ferrous and ferric Fe at depth for the autumn sampling period. **a.)** Peeper location A. **b.)** Peeper location B.

Discussion

In waters saturated with Fe, the pH and Fe concentration can largely be controlled by Fe mineral precipitation and dissolution (Le and Kim, 2008). Fe oxyhydroxides are common

secondary minerals within AMD that undergo dissolution at pH values less than 3.5 (Gunsinger et al., 2006b) and are most stable in oxic conditions at near neutral pH values (Rimstidt, 2009). This is consistent with geochemical modeling results of saturation indices that suggest Fe oxyhydroxides to be unstable thermodynamically in pore water collected at the study site in the summer sampling period due to the low pH. Some samples for both peeper locations A and B exhibited pH values above 3.5 for the autumn sampling period. The existence of such low pH values during the summer indicates Fe oxyhydroxide mineral dissolution has a minimal control on Fe concentrations and pH and that the oxidation of sulfide minerals is the major contributor to Fe and acidity within the refuse deposit. Lower pH values at the surface may indicate that acidity is being generated more rapidly there and that the acidic water is percolating down the soil profile and perhaps increasing in pH as a result of dilution as the water begins to intersect the water table. Acidity near the surface is also likely a result of evaporation within the upper portions of the profile, concentrating hydrogen ions in pore waters that become more dilute going down the soil profile (Nordstrom et al., 2000). The pH near the surface at peeper location A is less than that at the surface of peeper location B, suggesting that the extent of pyrite oxidation is greater at this location. Distinct pH zones occurring below the water table could also indicate low flow or stagnant groundwater conditions. The water table was relatively low during the summer (Fig. 2) allowing most of the profile to be exposed to unsaturated conditions.

At pH values less than 4.0, Fe^{3+} acts as the primary oxidant of pyrite and conditions exist that allow oxidizing bacteria to oxidize Fe^{2+}, a product of pyrite oxidation, to Fe^{3+} (Huminicki and Rimstidt, 2009). This leads to a cyclical positive feedback system that keeps pH values low. Such an occurrence at Minnehaha could allow for the pH of the refuse deposit to remain low at both saturated unsaturated conditions. If this is not occurring the depth of the unsaturated zone could be considered the main control on pyrite oxidation (Gunsinger et al., 2006a). Due to the shallow depth of the unsaturated zone, the soil development of the refuse deposit could be considered relatively immature due to low rates of acidity generation and the potential for higher rates if more of the refuse is exposed to atmospheric oxygen.

Inverted pH profiles at sampling location B during the autumn (Fig. 6b) in comparison to the summer (Fig. 4) is likely the result of downward flushing of the previously evaporatively concentrated pore waters of the upper part of the soil profile followed by dilution by rainwater near the surface during the wet season. This would allow for accumulation of acidity near the

bottom of the profile during the autumn as shown in Fig. 6. Calculations of potential evapotranspiration using Penman's equation and data from a nearby weather station support this. Potential evapotranspiration for the summer sampling period was 9.9 cm and 5.8 for the autumn, leaving a higher potential for concentration of evaporative salts and acidity concentration within the upper portions of the profile during the summer.

Ferrous iron is most stable below the zone of oxidation within refuse deposits while Fe^{3+} is rapidly generated from Fe^{2+} within zones of oxidation (Gunsinger et al., 2006b). Data from the autumn samples showing higher concentrations of Fe^{2+} at peeper location B and higher concentrations of Fe^{3+} at peeper location A may indicate that zones of oxidation exist within the refuse deposit. The presence of high concentrations of Fe^{2+} relative to Fe^{3+} within the saturated zone at peeper location A suggest that atmospheric oxygen is the main oxidant of Fe^{2+} within the refuse opposed to microbial oxidation. This is in agreement with water table data showing that the groundwater elevation is lower at peeper location A, where Fe^{3+} is the dominant Fe-species, than location B, allowing for more exposure to atmospheric oxygen to oxidize Fe^{2+}. Observations of increases in Fe^{3+} (Fig. 7a) concentration at both peeper locations A and B also appear to correlate with decreases in pH (Fig. 6a). This data suggests that Fe^{3+} is acting as an oxidant of pyrite along with atmospheric oxygen to generate acidity within the both the saturated and unsaturated zone.

Continued sampling under varying seasonal and hydrologic conditions is necessary to fully understand the oxidation pathways of the refuse deposit and the dynamics of pH under these conditions. The use of peepers allows a unique opportunity to obtain and analyze pore water samples for ions sensitive to redox conditions, such as Fe, arsenic (As), and sulfur species, with limited disturbance of samples from their original state. Future analyses will include concentrations of As species, As^{3+} and As^{5+}, through the use of the *Dionex© ICS-2000 Ion Chromatograph System*. Projected sampling events will also analyze both sulfate and sulfide concentrations in relation to the $\delta^{34}S$ values of each in an effort to identify zones of reduction within the depth profiles. The combinations of these data will allow for further quantification of zones of oxidation and reduction and the processes that drive them.

CONCLUSION

Preliminary findings that most of the acidity is generated at the top of the soil profile and percolates downward and that lower pH conditions existed during summer when the unsaturated zone was deeper are interpreted to indicate that atmospheric oxygen is the main source of pyrite oxidation within the refuse deposit. This is in conflict with data from peeper location A during the autumn that implies Fe^{3+} is playing a major role in pyrite oxidation within the refuse deposit. Based on the data showing that the main oxidant of Fe^{2+} is atmospheric oxygen within the unsaturated zone it can be concluded that both Fe^{3+} and atmospheric oxygen are contributing to oxidation of pyrite within the low pH environment but that the extent of Fe^{3+} is limited by exposure to atmospheric oxygen. Based on this conclusion, it is proposed for reclamation that the water table depth be increased, thus decreasing unsaturated zone thickness and minimizing further oxidation. Although there are obvious negative effects of the water table, such a manipulation would likely prevent a positive feedback cycle in which Fe^{2+} is allowed to be oxidized by atmospheric oxygen and producing Fe^{3+}. The Fe^{3+} could then potentially oxidize more pyrite, thereby creating further acidity. A more likely, and previously employed, manipulation is to temporarily add alkalinity to raise the pH to a value that allows the precipitation of Fe-bearing minerals on the surfaces of pyrite minerals. This tends to fix Fe concentrations and retard pyrite oxidation as the exposed surface of pyrite becomes covered by precipitated iron oxyhydroxides.

Acknowledgements

Funding for this project was provided from the Indiana Department of Natural Resources, Division of Reclamation. Special thanks go to Jack Hadden of the Indiana Geological Survey, Center for Geospatial Data Analysis, for technical assistance during the collection of hydrologic data throughout the study period.

Bibliography

Fortin, D., Goulet, R., and Roy, M., 2000. Seasonal Cycling of Fe and S in a Constructed inWetland: The Role of Sulfate-Reducing Bacteria. Geomicrobiology Journal 17, 221-235. http://dx.doi.org/10.1080/01490450050121189.

Gunsinger, M.R., Ptacek, C.J., Blowes, D.W., and Jambor, J.L., 2006a. Evaluation of long-term sulfide oxidation processes within pyrrhotite-rich tailings, Lynn Lake, Manitoba.Contaminate Hydrology 83, 159-170. http://dx.doi.org/10.1016/j.jconhyd.2005.10.0130.

Gunsinger, M.R., Ptacek, C.J., Blowes, D.W., Jambor, J.L., and Moncur, M.C., 2006b. Mechanisms controlling acid neutralization and metal mobility within a Ni-rich tailings impoundment. Applied Geochemistry 21, 1301-1321. http://dx.doi.org/10.1016/j.apgeochem.2006.06.006.

Huminicki, D.M.C and Rimstidt, J.D., 2009. Iron oxyhydroxide coating of pyrite for acid mine drainage control. Applied Geochemistry 24, 1626-1634. http://dx.doi.org/10.1016/j.apgeochem.2009.04.032.

Jerz, J.K. and Rimstidt, J.D., 2004. Pyrite oxidation in moist air. Geochimica et Cosmochimica Acta 68, 701-714. http://dx.doi.org/10.1016/S0016-7037(03)00499-X.

Lee, J. and Kim, Y., 2008. A quantitative estimation of the factors affecting pH changes using simple geochemical data from acid mine drainage. Environ Geol 55, 65-75. http://dx.doi.org/10.1007/s00254-007-0965-6.

Nordstrom, D.K., Alpers, C.N., Ptacek, C.J., and Blowes, D.W., 2000. Negative pH and extremely acidic mine water from Iron Mountain, California. Envionmental Science and Technology 34: 254-258. http://dx.doi.org/10.1021/es990646v.

Parkhurst, D. and Appelo, C.A.J., 1999. User's guide to PHREEQC (Version 2) --- A compute program for speciation, batch-reaction, one dimensional transport, and inverse geochemical calculations. U.S. Geological Survey-Resources Investigations Report 99-4259, 310.

Smith, J. and Melville, M.D., 2004. Iron monosulfide formation and oxidation in drain-bottom sediments of an acid sulfate soil environment. Applied Geochemistry 19, 1837-1853. http://dx.doi.org/10.1016/j.apgeochem.2004.04.004.

White, P.V.O., Macdonald, B.C.T., Ford, P., and Melville, M.D., 2008. The use of peepers to sample pore water in acid sulphate soils. European Journal of Soil Science 59, 762-770. http://dx.doi.org/10.1111/j.1365-2389.2008.01020.x.

Williamson, M.A., and Rimstidt, J.D., 1994. The kinetics and electrochemical rate-determining step of aqueous pyrite oxidation. Geochimica et Cosmochimica Acta 58, 5443-5454. http://dx.doi.org/10.1016/0016-7037(94)90241-0.